一般社団法人　電子情報通信学会
THE INSTITUTE OF ELECTRONICS,
INFORMATION AND COMMUNICATION ENGINEERS

信学技報
IEICE Technical Report
SR2018-88 (2018-10)

[Poster Presentation] Neural Network-based Channel Occupancy Rate Prediction

Hiroki IWATA†, Kenta UMEBAYASHI†, Ahmed AL-TAHMEESSCHI††, and Miguel LÓPEZ-BENÍTEZ††

† Department of Electrical and Electronic Engineering, Tokyo University of Agriculture and Technology, 2–24–16 Naka-cho, Koganei-shi, Tokyo, 184–8588 Japan

†† Department of Electrical Engineering and Electronics, University of Liverpool, Merseyside, L69 3GJ, United Kingdom

E-mail: iwa-hiro@st.go.tuat.ac.jp

Abstract A spectrum occupancy prediction can provide useful information to spectrum sharing-based wireless networks. In this paper, we investigate a neural network-based channel occupancy rate prediction. Specifically, based on real occupancy rate data obtained by our spectrum measurement system, we reveal a relationship between the prediction performance and several neural network parameters, such as the number of hidden layers and the number of units in each hidden layer. Numerical evaluation shows an advantage of the neural network-based prediction by comparing with other prediction methods, such as autoregressive model.

Key words COR Prediction, Dynamic Spectrum Access, Smart Spectrum Access, Spectrum Measurement

1. Introduction

Due to fixed spectrum assignment policy and increasing demand of wireless communications, spectrum becomes a scarce natural resource and there is little room to accommodate new wireless systems [1]. However, several spectrum measurement campaigns around the world [2–5] have shown that almost all the spectrum is under-utilized in terms of time and space [6, 7]. It means there are a lot of unused spectrum, which is called white space (WS). For this issue, dynamic spectrum access (DSA) has been investigated [8].

In DSA, there are primary users (PUs), which have priority regarding spectrum usage, and secondary users (SUs), which can opportunistically access the vacant spectrum as long as the spectrum utilization by SUs does not cause any harmful interference to PUs.

In DSA, SUs have to detect WS to protect PUs from the harmful interference. Moreover, instantaneous information of the target spectrum, either vacant or occupied, is necessary to share the spectrum with PUs whose spectrum utilization may change dynamically. Spectrum sensing is a technique to find WS [9]. However, requirements of spectrum sensing, such as accuracy, latency and implementation cost in DSA are substantially high. For small and low cost mobile terminal, low implementation cost and energy efficient scheme for spectrum sensing is also required [10].

Not only to resolve the issue of spectrum sensing but also to provide other benefits to DSA, advanced DSA, known as smart spectrum access (SSA), has been investigated [11–13]. SSA exploits useful prior information in terms of PU's spectrum usage. This information can be obtained by long-term, broadband and wide area spectrum usage measurements and this information can be used to achieve efficient spectrum sharing smartly. In fact, it has been shown that channel occupancy rate (COR) information can enhance spectrum sensing performance [14–16]. It can also enhance spectrum management, channel selection, MAC protocol for DSA [17–19].

So far, models of spectrum occupancy have been widely investigated, for example in [20–22]. On the other hand, spectrum occupancy prediction is a new approach compared to spectrum sensing and spectrum occupancy modeling [23–25]. Spectrum occupancy prediction infers future spectrum occupancy from the measured spectrum usages. Spectrum occupancy prediction has many merits such as reducing sensing time and energy consumption involved in spectrum sensing and increasing system throughput, and so on [26].

There are three widely used prediction methods in spectrum occupancy prediction, linear prediction such as autoregressive (AR) model, moving average model, hidden Markov models and artificial neural networks (ANN) [23]. There

are excellent survey papers which comprehensively summarize spectrum occupancy prediction techniques, for example, [23–25]. Among them, ANN-based prediction is a promising approach due to the success of deep learning (or deep neural network) in industrial and academic field with the development of computing power and the arrival of big data era [27]. Moreover, [28] shows a recurrent neural network-based spectrum occupancy prediction generally exhibits the highest accuracy among the other methods such as AR model and support vector machine. In recent years, ANN and deep learning have also received significant attention in wireless communication field [29, 30]. ANN is models that attempt to mimic some of the basic information processing methods found in the brain and a kind of machine learning technology [31].

This paper focuses on COR prediction problem based on ANN in SSA. The performance of ANN-based prediction depends on the model structure of the network (e.g., number of layers and neurons) [32]. Thus, it is important to reveal a relationship between the performance of COR prediction and several ANN model parameters, such as the number of hidden layers and the number of neurons in each hidden layer. The main contributions of this paper are as follows:

- We reveal the relationship between the the performance of COR prediction and several ANN model parameters based on real COR data obtained by our developed spectrum occupancy measurement system.
- Numerical evaluations show the importance of input size to the designed network rather than the number of hidden layers and the number of neurons. This gives our the insight into to the design criterion of network architecture for COR prediction.

The rest of the paper is organized as follows: Section 2. presents several related works with respect to ANN-based spectrum occupancy prediction. Section 3. formulates the COR prediction problem and presents the COR prediction framework in SSA. Section 4. is devoted for the description of spectrum usage measurement methodology and COR estimation process. In Section 5., the assumed ANN model in this work is shown. The numerical evaluation and its corresponding discussion are provided in Section 6. Finally, Section 7. gives the conclusion of the paper and points out the future work.

2. Related Work

In this section, we introduce several ANN-based spectrum occupancy prediction techniques, especially feed-forward neural network-based prediction techniques due to its popularity. In [23, 25], more detailed survey is conducted.

An ANN-based spectrum occupancy prediction learns the PUs' spectrum occupancy via the learning process, and then predicts the future spectrum occupancy. In feed-forward neural networks, the input data (binary sequences for spectrum occupancy state) are input to the input layer and the predicted value (or values) are output from the output layer via the hidden layers without any feedback. There are several works which apply feed-forward neural network to predict the spectrum occupancy, for example [33], [34] and [35], etc.

In [33], the simplest feed-forward neural network, multilayer perception (MLP), is applied to spectrum occupancy prediction. Specifically, authors in [33] designed an MLP consisted of one input layer with 4 inputs, two hidden layers with 15 neurons in the first layer and 20 neurons in the second layer and one output layer. Moreover, they used the batch back propagation algorithm, which can minimize the mean square error between the output from the MLP and the desired value and is based on gradient descent algorithm to train the MLP. They showed the spectrum occupancy prediction based on MLP can save the sensing energy and improve the efficiency of spectrum access by SUs.

[34] showed with the soft information (i.e., power information) instead of hard information (binary spectrum occupancy state information) as the input data to the backpropagation neural network, the prediction performance can be improved than hard decision spectrum prediction. Furthermore, authors in [34] extended their work to improve the prediction performance in [35]. Specifically, they applied the genetic algorithm for searching for the optimal parameters such as weights and the momentum algorithm for faster and stable training.

Note that the above mentioned works focus on predicting the binary spectrum occupancy state (whether a channel is busy or idle in the upcoming next time slot). On the other hand, we focus on COR prediction based on ANN in this paper, where COR indicates the fraction of time that the channel is declared to be busy.

3. COR Prediction in SSA

3. 1 COR Prediction Framework in SSA

In this subsection, at first we introduce the concept of SSA, then present a framework of COR prediction in SSA concretely. Figure 1 shows the conceptual diagram of SSA. SSA consists of two layers, DSA layer (upper layer in Fig. 1) and spectrum awareness layer (lower layer in Fig. 1). DSA layer consists of primary system and DSA system and dynamic spectrum sharing between PUs and SUs is achieved in this layer. The distinct feature of SSA from typical DSA is that the DSA system smartly shares the spectrum with primary system exploiting useful information regarding spectrum us-

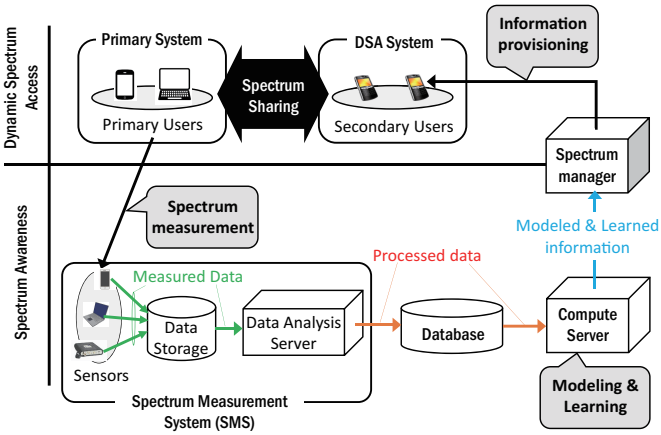

Fig. 1 Conceptual diagram of SSA & framework of COR prediction

age by PUs. These useful information are provided by the spectrum manager, which is an interface between DSA layer and spectrum awareness layer.

On the other hand, spectrum awareness layer is responsible for spectrum usage measurements, measured data analysis and useful information provisioning to the DSA system. The spectrum awareness layer consists of spectrum measurement system (SMS), database and compute server.

A spectrum measurement system is composed of several spectrum sensors such as spectrum analyzer and smart phone, data analysis server and data storage. Sensors collect the source data for useful statistical information such as I/Q data and send the source data to the data storage. The data analysis server processes the collected data by sensors and estimates statistical information based on the processed data. Finally, estimated statistical information are stored in the database.

The compute server is responsible for modeling and learning of statistical information. The spectrum manager extracts useful information based on modeled or learned information by the compute server and provides extracted information to the DSA system.

Now, we move on the COR prediction framework in SSA. The COR prediction consists of three main blocks, spectrum measurement and COR estimation block, predictor learning block and prediction block. The spectrum measurement and COR estimation block is performed in SMS in spectrum awareness layer. Estimated CORs are stored in the database. In Section 4., we will show the developed spectrum measurement system prototype and COR estimation process.

The pedictor leaning is responsible for the predictor generation based on the estimated CORs stored in the database. This includes the determination of the predictor model used and the estimation of predictor parameters. This process is performed in the compute server in Fig. 1.

Finally, prediction is performed based on the learned predictor and the COR data from SUs. The predictor is constructed in the spectrum manager. Thus, SUs in DSA system provide the COR data on demand to the spectrum manager, then the predictor predicts the future COR value. The spectrum manager returns the predicted COR values back to the corresponding SUs.

3. 2 COR Prediction Problem Formulation

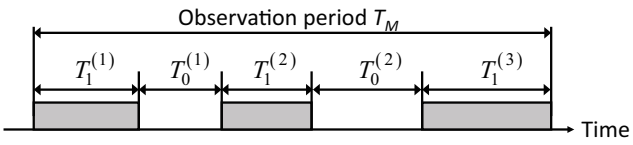

Fig. 2 COR for a Channel

In this subsection, we define COR and formulate a COR prediction problem.

COR at time instant t, $\Psi(t)$ is defined as the ratio of occupied time length by a channel to an observation period, T_M. For an example in Fig. 2, we can ideally calculate the COR as $\Psi(t) = \frac{1}{T_M}\sum_{i=1}^{3} T_1^{(i)}$, where T_1 and T_0 mean the occupied time length and the unoccupied time length (i.e., WS), respectively. Practically, we must estimate the COR and then consider its estimated COR as the true COR $\Psi(t)$ since we do not know the true COR. In Sect. 4., we will explain the COR estimation process based on spectrum measurement in this work.

Then, we can formulate the (one-step ahead) COR prediction problem as follows: Given a time series data regarding COR up to current time t, $\mathbf{\Psi}(t)$, we predict the future COR value at time instant $t+1$, $\hat{\Psi}(t+1)$ as

$$\hat{\Psi}(t+1) = g(\mathbf{\Psi}(t)), \tag{1}$$

where $\mathbf{\Psi}(t) = [\Psi(t-\tau+1), \ldots, \Psi(t-1), \Psi(t)]^T$ and τ and ^{T} indicate the time delay lag and the transpose operation. Moreover, $g(\cdot)$ presents a learned linear or nonlinear function which expresses a relationship between the input $\mathbf{\Psi}(t)$ and the output $\hat{\Psi}(t+1)$.

From a perspective of SSA, $\mathbf{\Psi}(t)$ is given by any SUs on demand, while the function $g(\cdot)$ and corresponding model parameters are learned/estimated by the compute server. The predicted COR, $\hat{\Psi}(t+1)$ is predicted by the spectrum manager and provided to SUs.

COR prediction aims to achieve the prediction error between the true COR, $\Psi(t+1)$ between $\hat{\Psi}(t+1)$ as small as possible. In this work, we apply RMSE (root mean square error) as the prediction error given by (2).

$$\mathrm{RMSE}(\Psi) = \sqrt{\frac{1}{T}\sum_{t=1}^{T}(\hat{\Psi}(t+1) - \Psi(t+1))^2}, \tag{2}$$

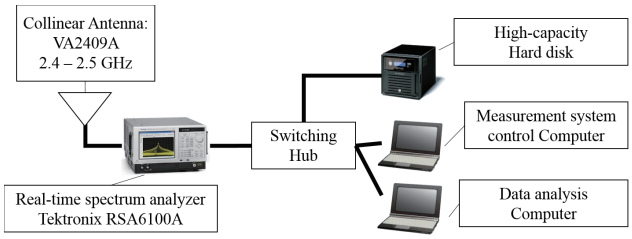

Fig. 3 Spectrum measurement system prototype

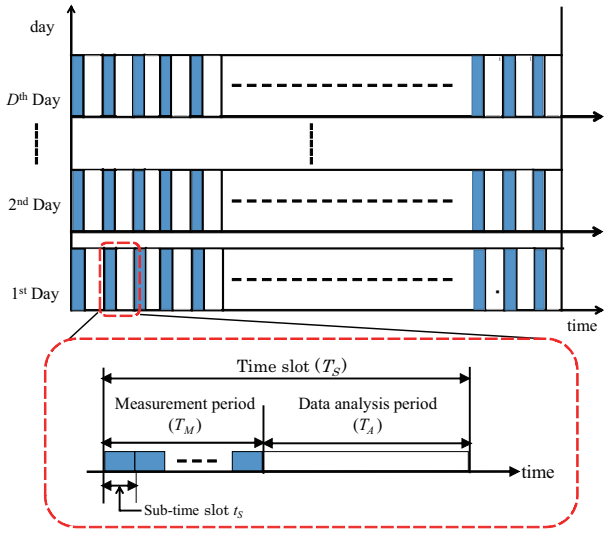

Fig. 4 Measurement time schedule

where T indicates the total number of COR samples exploited for prediction.

4. Measurement Setup and Methodology

The measurement setup and methodology to obtain COR data for learning ANN models are shown in this section. We performed a spectrum usage measurement campaign in the frequency band is 2.4 GHz (the center frequency is 2437 MHz and the bandwidth is 1.25 MHz). The spectrum measurement system (SMS) prototype is located in our laboratory on fourth floor of a building in Koganei-campus, Tokyo University of Agriculture and Technology, Tokyo, Japan (35°41'55.8"N 139°31'00.6"E).

The block diagram of the SMS prototype is shown in Fig. 3. The system prototype consists of an antenna that can observe the target frequency band, cables, a real-time spectrum analyzer (RSA) (Tektronix RSA6100A), a network-attached high-capacity hard disk, a measurement system manager, and a data analysis computer.

The measurement system manager takes care of the measurement time scheduling, which is shown in Fig. 4. The number of days for spectrum measurement is denoted by D and we set $D = 24$ in the spectrum usage measurement. One day (24 hours) is divided into M time slots. The time duration for one time slot is denoted by T_S and we set T_S to 5 seconds. This means the spectrum manager predicts the COR 5 seconds ahead given the measured COR data by any SUs. One time slot consists of a measurement period and a data analysis period, whose time durations are denoted by T_M and T_A, respectively. During one measurement period, the RSA continuously observes the target frequency band for T_M seconds and we set $T_M = 250$ ms in this measurement (i.e., $T_A = 4.75$ sec).

The measured data (I/Q data in this spectrum usage measurement) is first stored in the hard disk and then transferred to the data analysis computer. The data analysis computer provides estimates of the COR by means of Welch fast Fourier transform-based energy detection (Welch FFT-ED) and post processing to achieve accurate spectrum usage detection performance [12]. The measurement period T_M is divided into N_T sub-time slots and Welch FFT-ED is performed in each sub-time slot. The time duration for one sub-time slot is denoted by t_S. There are N_S I/Q data samples and N_F frequency bins in one sub-time slot.

The spectrum usage detections are performed based on the $N_T \times N_F$ estimated power spectrum samples by Welch FFT at the data analysis computer. In this measurement, the spectrum usage detections consists of typical ED and signal area estimation with false alarm cancellation [12]. The parameters for the Welch FFT-ED are as follows: In Welch FFT, 512 I/Q data samples ($N_S = 512$) are divided into 7 segments while the overlap ratio is set to 0.5 [36]. Therefore, the number of frequency bins, N_F are set to 128 and 7 estimated power spectra with 128 frequency bins are averaged, leading to one estimated power spectrum by Welch FFT. We set the detection threshold based on constant false alarm rate criterion where the target false alarm rate is set to 0.01. In this criterion, we need noise floor information in order to set the threshold and we employ forward consecutive mean excision (FCME) algorithm for noise floor estimation [37,38].

The outputs of the spectrum usage detection at time instant t are denoted by

$$D_{n_T,n_F} = \begin{cases} 1 & \text{(spectrum is occupied)} \\ 0 & \text{(spectrum is vacant),} \end{cases} \tag{3}$$

where n_T is the sub-time slot index number and n_F is the frequency bin index number. We define a set of index numbers of frequency bin, n_F, involved in the observed frequency band as $\mathbf{F}$, which corresponds to one channel. Then, the COR in the channel at time instant t can be estimated by

$$\Psi_d(t) = \frac{1}{N_T} \sum_{n_T} \left(1 - \prod_{n_F \in \mathbf{F}} (1 - D_{n_T,n_F}) \right). \tag{4}$$

This equation indicates that if a part of the target channel $\mathbf{F}$ is occupied, the state of the whole target channel is detected

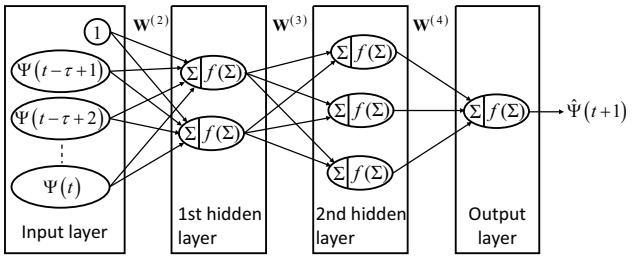

Fig. 5 Feed-forward neural network model

as occupied as well.

5. ANN-based COR Prediction

ANNs consist of a set of interconnected neurons and it typically has layered architecture (i.e., input layer, several hidden layers and output layer) as shown in Fig. 5. ANN has the capacity to learn and model complex nonlinear relationships [31]. Furthermore, ANNs are classified according to its model structure as the feed-forward neural network (e.g., multilayer perception and back propagation neural network) and recurrent neural network (e.g., Elman recurrent neural network, echo state network and long short-term memory). Generally, the parameters of ANNs (i.e., weights which determine the degree of connection among neurons) are learnt via gradient descent algorithm in the predictor learning. We focus on a feed-forward neural network as the network model in this work.

Figure 5 shows an example of the feed-forward neural network model applied in this work. The input data corresponds to $\mathbf{\Psi}(t)$ in (1) and the output corresponds to $\hat{\Psi}(t+1)$ in (1). Each neuron receives one or more inputs from one preceding layer, calculates their weighted sum, and finally outputs a non-linearly processed weighted sum. Specifically, this operation is given by

$$\begin{cases} u &= w_1x_1 + w_2x_2 + \cdots + w_Nx_N + b = \mathbf{w}^T\mathbf{x} + b, \\ z &= f(u), \end{cases} \tag{5}$$

where u presents the value of weighted sum of inputs from one preceding layer, $\mathbf{x} = [x_1, x_2, \ldots, x_I]^T$, while b indicates the bias term. $\mathbf{w} = [w_1, w_2, \ldots, w_N]^T$ and N indicate the weight vector and the number of inputs from one preceding layer (equivalently the number of weights), respectively. z is the output from a neuron where $f(\cdot)$ indicates a nonlinear function called activation function. There exist several widely used activation functions, such as logistic sigmoid functions, hyperbolic tangent function, rectified linear function and identity function, etc.

Therefore, we can express the input-output relation of lth layer ($l \in \{2, 3, \ldots, L\}$) as (6), where L presents the number of layers in the considered ANN model. In Fig. 5, the number of layers is $L = 4$.

$$\begin{cases} \mathbf{u}^{(l)} &= \mathbf{W}^{(l)}\mathbf{x}^{(l-1)} + \mathbf{b}^{(l)}, \\ \mathbf{z}^{(l)} &= \mathbf{f}^{(l)}(\mathbf{u}^{(l)}), \end{cases} \tag{6}$$

where $\mathbf{W}^{(l)} = [\mathbf{w}_{1,l}^T, \mathbf{w}_{2,l}^T, \cdots, \mathbf{w}_{J_{(l)},l}^T]^T$ indicates the weight matrix of lth layer. $\mathbf{w}_{j,l}$ ($j \in \{1, 2, \ldots, J_{(l)}\}$, $l \in \{2, 3, \ldots, L\}$) corresponds to the weight vector for jth neuron in lth layer where $J_{(l)}$ indicates the number of outputs from $l-1$th layer (corresponding to the number of inputs of lth layer). In Fig. 5, $J_{(2)} = \tau = 3$, $J_{(3)} = 2$, $J_{(4)} = 3$, respectively. $\mathbf{x}^{(l)}$ is the input vector to lth layer (equivalently output vector from $l-1$th layer). $\mathbf{f}^{(l)}(\cdot)$ is an element-wise activation function.

Finally, we can express the input-output relation of ANN model for COR prediction as (7) at the top of next page.

For constructing the ANN, we need to determine the number of hidden layers L, the number of neurons in each layer $J(l), l = 2, \ldots, L$ and input size τ to the ANN before the weight learning (estimation). However, it is difficult to optimally determine them since they are data-specific. For this issue, we investigate the relationship between the prediction performance and the above mentioned parameters based on real COR data obtained by our spectrum measurement system, which was described in Section. 4..

6. Numerical Evaluation

In this section, we present several relationships between the prediction performance evaluated by (2) and several ANN model parameters. These relationships are based on real COR data obtained by an SMS prototype described in Section. 4.. Throughout this section, we focus on one-step ahead prediction, i.e., prediction of COR at time instant $t+1$, $\hat{\Psi}(t+1)$, using $\mathbf{\Psi}(t)$. Thus, the number of neuron in output layer is one. We apply the hyperbolic tangent sigmoid function and the identity function in hidden layer and output layer as the activation function, respectively. Levenberg-Marquardt algorithm are used as learning method. Moreover, we use the cross validation method in which the ratio of the training test data size to the test data size is 7 : 3.

Figure 6 shows RMSE(Ψ) as a function of the number of lag (τ). In this result, we use one hidden layer, i.e., $L = 3$ and the number of neurons in the hidden layer are set to $J(2) \in \{1, 30\}$. As you can see, increasing τ and the number of neurons result in smaller RMSE performance. Moreover, we can get a higher gain when increasing τ than when increasing the number of neurons.

Figure 7 shows the result of RMSE(Ψ) as a function of the number of neurons in hidden layer. In this result, we set the number of lag τ, the number of layers L to $\tau \in \{1, 2, 10, 100\}$ and $L = 3$, i.e., one hidden layer, respectively. From this

$$\hat{\Psi}(t+1) = \mathbf{z}^{(L)},$$
$$= \mathbf{f}^{(L)}(\mathbf{W}^{(L)}\mathbf{f}^{(L-1)}(\mathbf{W}^{(L-1)}\cdots\mathbf{f}^{(2)}(\mathbf{W}^{(2)}\mathbf{\Psi}(t)+\mathbf{b}^{(2)})\cdots+\mathbf{b}^{(L-1)})+\mathbf{b}^{(L)}). \quad (7)$$

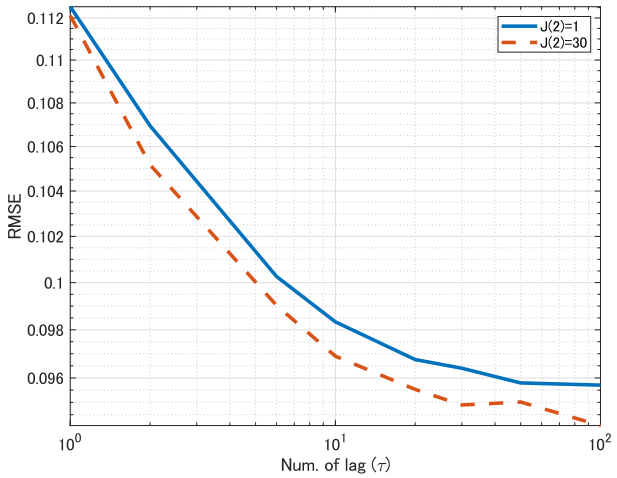

Fig. 6 Predictive RMSE vs. Number of lag (τ)

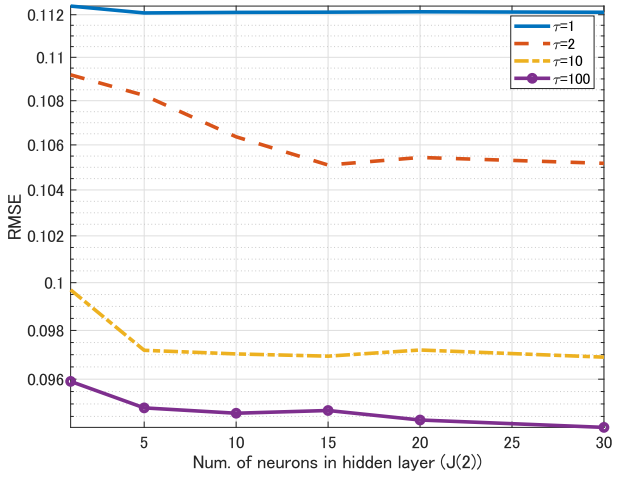

Fig. 7 Predictive RMSE vs. Number of neurons in hidden layer. $\tau \in \{1, 2, 10, 100\}$, $L = 3$, $J(2) \in \{1, 5, 10, 15, 20, 30\}$.

figure, we can see increasing the number of neurons in hidden layer, $J(2)$ may not an effective means since almost same performances are achieved even if increasing the number of neurons. On the other hand, increasing τ leads to a high gain in terms of RMSE performance. Thus, we can conclude it is beneficial for ANN design for COR prediction to increase τ.

Finally, we compare RMSE(Ψ) for several prediction methods in Fig. 8. We applied two comparative methods, AR model-based COR prediction and AR model with state change detection-based COR prediction [39]. In this result, we set the AR order parameter of both comparative methods to one as the authors in [39] confirmed the value is a proper value by extensive numerical evaluations. On the other hand,

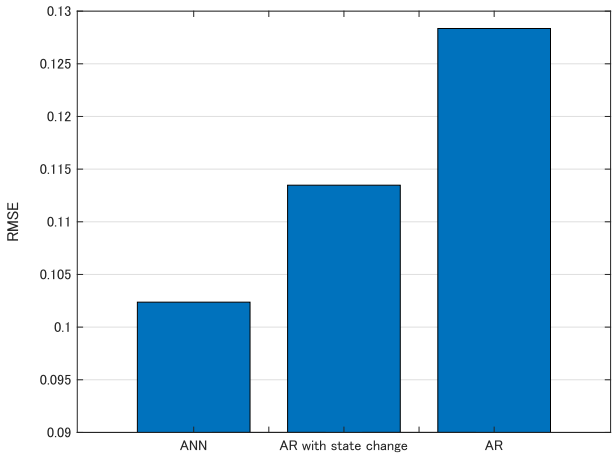

Fig. 8 Comparison of Predictive RMSE for several prediction methods.

we use one hidden layer, i.e., $L = 3$ and, the number of lag, τ and the number of neurons in hidden layer, $J(2)$ are set to $\tau = 10$ and $J(2) = 10$, respectively. Obviously, ANN-based COR prediction achieves the best RMSE performance. The analysis of the cause that why ANN-based COR prediction can achieve the best performance will be one of our future works.

7. Conclusion

In this paper, we investigate the ANN-based COR prediction. In ANNs, it is important to set the network parameters such as weight values and the number of layers appropriately. For this issue, we reveal the relationship between the prediction performance and several neural network parameters, such as the number of hidden layers and the number of units in each hidden layer based on COR data obtained by our spectrum measurement system. Numerical evaluations show the importance of input size to the designed network rather than the number of hidden layers and the number of neurons. This gives our the insight into to the design criterion of network architecture. Based on this insight, we will design the input data form and the number of input layer as a future work. Furthermore, we will consider other networks model such as recurrent neural network model and convolutional neural network model.

Acknowledgements

This work was supported by the European Commission

in the framework of the H2020-EUJ-02-2018 project 5G-Enhance (Grant agreement no. 815056) and the Ministry of Internal Affairs and Communications (MIC) of Japan and the JSPS KAKENHI Grant Numbers JP18K04124.

文　献

[1] J. Reed, M. Vassiliou, and S. Shah, "The role of new technologies in solving the spectrum shortage [point of view]," *Proc. IEEE*, vol. 104, no. 6, pp. 1163–1168, June 2016.

[2] J. Naganawa, H. Kim, S. Saruwatari, H. Onaga, and H. Morikawa, "Distributed spectrum sensing utilizing heterogeneous wireless devices and measurement equipment," in *Proc. IEEE DySPAN*, May 2011, pp. 173–184.

[3] T. M. Taher, R. B. Bacchus, K. J. Zdunek, and D. A. Roberson, "Long-term spectral occupancy findings in Chicago," in *Proc. IEEE DySPAN*, May 2011, pp. 100–107.

[4] V. Valenta, R. Maršálek, G. Baudoin, M. Villegas, M. Suarez, and F. Robert, "Survey on spectrum utilization in Europe: Measurements, analyses and observations," in *Proc. IEEE CROWNCOM*, June 2010, pp. 1–5.

[5] S. Yin, D. Chen, Q. Zhang, M. Liu, and S. Li, "Mining spectrum usage data: A large-scale spectrum measurement study," *IEEE Trans. Mobile Comput.*, vol. 11, no. 6, pp. 1033–1046, June 2012.

[6] D. Das and S. Das, "A survey on spectrum occupancy measurement for cognitive radio," *Springer Wireless Pers. Commun.*, vol. 85, no. 4, pp. 2581–2598, 2015.

[7] M. Höyhtyä, A. Mämmelä, M. Eskola, M. Matinmikko, J. Kalliovaara, J. Ojaniemi, J. Suutala, R. Ekman, R. Bacchus, and D. Roberson, "Spectrum occupancy measurements: A survey and use of interference maps," *IEEE Commun. Surveys Tuts*, vol. 18, no. 4, pp. 2386–2414, Fourth quarter 2016.

[8] Q. Zhao and B. M. Sadler, "A survey of dynamic spectrum access," *IEEE Signal Process. Mag.*, vol. 24, no. 3, pp. 79–89, May 2007.

[9] T. Yücek and H. Arslan, "A survey of spectrum sensing algorithms for cognitive radio applications," *IEEE Commun. Surveys Tuts.*, vol. 11, no. 1, pp. 116–130, First quarter 2009.

[10] G. Ding, J. Wang, Q. Wu, Y. Yao, F. Song, and T. A. Tsiftsis, "Cellular-base-station-assisted device-to-device communications in TV white space," *IEEE J. Sel. Areas Commun.*, vol. 34, no. 1, pp. 107–121, Jan. 2016.

[11] K. Umebayashi, S. Tiiro, and J. J. Lehtomäki, "Development of a measurement system for spectrum awareness," in *Proc. IEEE 5GU*, Nov. 2014, pp. 234–239.

[12] K. Umebayashi, K. Moriwaki, R. Mizuchi, H. Iwata, S. Tiiro, J. J. Lehtomäki, M. López-Benítez, and Y. Suzuki, "Simple primary user signal area estimation for spectrum measurement," *IEICE Trans. Commun*, vol. E99-B, no. 8, pp. 523–532, Feb. 2016.

[13] T. Fujii and K. Umebayashi, "Smart spectrum for future wireless world," *IEICE Trans. Commun.*, vol. E100-B, no. 9, pp. 1661–1673, Sep. 2017.

[14] N. Wang, Y. Gao, and X. Zhang, "Adaptive spectrum sensing algorithm under different primary user utilizations," *IEEE Commun. Lett.*, vol. 17, no. 9, pp. 1838–1841, Sept. 2013.

[15] T. Nguyen, B. L. Mark, and Y. Ephraim, "Spectrum sensing using a hidden bivariate Markov model," *IEEE Trans. Wireless Commun.*, vol. 12, no. 9, pp. 4582–4591, Sept. 2013.

[16] K. Umebayashi, K. Hayashi, and J. J. Lehtomäki, "Threshold-setting for spectrum sensing based on statistical information," *IEEE Commun. Lett.*, vol. 21, no. 7, pp. 1585–1588, Apr. 2017.

[17] M. Wellens, J. Riihijarvi, and P. Mahonen, "Evaluation of adaptive MAC-layer sensing in realistic spectrum occupancy scenarios," in *Proc. IEEE DySPAN*, Apr. 2010, pp. 1–12.

[18] K. Umebayashi, Y. Suzuki, and J. J. Lehtomäki, "Dynamic selection of CWmin in cognitive radio networks for protecting IEEE 802.11 primary users," in *Proc. IEEE CROWNCOM*, June 2011, pp. 266–270.

[19] Y. Xu, A. Anpalagan, Q. Wu, L. Shen, Z. Gao, and J. Wang, "Decision-theoretic distributed channel selection for opportunistic spectrum access: Strategies, challenges and solutions," *IEEE Commun. Surveys Tuts.*, vol. 15, no. 4, pp. 1689–1713, Fourth quarter 2013.

[20] M. López-Benítez and F. Casadevall, "Empirical time-dimension model of spectrum use based on a discrete-time Markov chain with deterministic and stochastic duty cycle models," *IEEE Trans. on Veh. Technol.*, vol. 60, no. 6, pp. 2519–2533, July 2011.

[21] Y. Chen and H. Oh, "A survey of measurement-based spectrum occupancy modeling for cognitive radios," *IEEE Commun. Surveys Tuts*, vol. 18, no. 1, pp. 848–859, First quarter 2016.

[22] K. Umebayashi, M. Kobayashi, and M. López-Benítez, "Efficient time domain deterministic-stochastic model of spectrum usage," *IEEE Trans. Wireless Commun.*, vol. 17, no. 3, pp. 1518–1527, Mar. 2018.

[23] G. Ding, Y. Jiao, J. Wang, Y. Zou, Q. Wu, Y. Yao, and L. Hanzo, "Spectrum inference in cognitive radio networks: Algorithms and applications," *IEEE Commun. Surveys Tuts.*, vol. 20, no. 1, pp. 150–182, First quarter 2018.

[24] X. Xing, T. Jing, W. Cheng, Y. Huo, and X. Cheng, "Spectrum prediction in cognitive radio networks," *IEEE Wireless Commun.*, vol. 20, no. 2, pp. 90–96, Apr. 2013.

[25] S. E. R. J. L. Y. C. R. B. Eltom, Hamidand Kandeepan, "Statistical spectrum occupancy prediction for dynamic spectrum access: a classification," *EURASIP J. Wireless Commun. Netw.*, vol. 2018, no. 1, p. 29, Feb. 2018.

[26] G. Ding, J. Wang, Q. Wu, Y. Yao, R. Li, H. Zhang, and Y. Zou, "On the limits of predictability in real-world radio spectrum state dynamics: from entropy theory to 5g spectrum sharing," *IEEE Commun. Mag.*, vol. 53, no. 7, pp. 178–183, July 2015.

[27] Y. LeCun, Y. Bengio, and G. Hinton, "Deep learning," *Nature*, no. 1, pp. 436–444, May 2015.

[28] A. Agarwal, A. S. Sengar, and R. Gangopadhyay, "Spectrum occupancy prediction for realistic traffic scenarios: Time series versus learning-based models," *Springer J. Commun. Inf. Netw.*, vol. 3, no. 2, pp. 44–51, Jun. 2018.

[29] T. O'Shea and J. Hoydis, "An introduction to deep learning for the physical layer," *IEEE Trans. Cogn. Commun. Netw.*, vol. 3, no. 4, pp. 563–575, Dec. 2017.

[30] T. Wang, C.-K. Wen, H. Wang, F. Gao, T. Jiang, and S. Jin, "Deep learning for wireless physical layer: Opportunities and challenges," *China Commun.*, vol. 14, no. 11, pp. 92–111, Nov. 2017.

[31] S. Samarasinghe, *Neural Networks for Applied Sciences and Engineering*. Boston, MA, USA: Auerbach Publications, 2006.

[32] Y. Zhao, Z. Hong, Y. Luo, G. Wang, and L. Pu, "Prediction-based spectrum management in cognitive radio networks," *IEEE Syst. J.*, pp. 1–12, 2018.

[33] V. K. Tumuluru, P. Wang, and D. Niyato, "Channel status prediction for cognitive radio networks," *Wireless Commun. and Mobile Comput.*, vol. 12, no. 10, pp. 862–874, 2012.

[34] S. Bai, X. Zhou, and F. Xu, ""soft decision" spectrum prediction based on back-propagation neural networks," in *Proc. IEEE ComManTel*, Apr. 2014, pp. 128–133.

[35] ——, "Spectrum prediction based on improved-back-

propagation neural networks," in *Proc. IEEE ICNC*, Aug. 2015, pp. 1006–1011.

[36] P. D. Welch, "The use of fast Fourier transform for the estimation of power spectra: A method based on time averaging over short, modified periodograms," *IEEE Trans. Audio Electroacoust.*, vol. 15, no. 2, pp. 70–73, June 1967.

[37] J. J. Lehtomäki, R. Vuohtoniemi, and K. Umebayashi, "On the measurement of duty cycle and channel occupancy rate," *IEEE J. Sel. Areas Commun.*, vol. 31, no. 11, pp. 2555–2565, Nov. 2013.

[38] K. Umebayashi, R. Takagi, N. Ioroi, Y. Suzuki, and J. J. Lehtomäki, "Duty cycle and noise floor estimation with Welch FFT for spectrum usage measurements," in *Proc. IEEE CROWNCOM*, June 2014, pp. 73–78.

[39] D. Cho, K. Umebayashi, S. Narieda, and M. López-Benítez, "A study on time series modeling of duty cycle for smart spectrum access," in *IEICE Tech. Rep.*, Feb. 2018, pp. 1–7.